ORIGINAL ARTICLE

Causative role for defective expression of mitochondria-eating protein in accumulation of mitochondria in thyroid oncocytic cell tumors

Zhanna Mussazhanova[1,2] | Mika Shimamura[3] | Tomomi Kurashige[3] | Masahiro Ito[4] |
Masahiro Nakashima[1] | Yuji Nagayama[3] iD

[1]Department of Tumor and Diagnostic
Pathology, Atomic Bomb Disease Institute,
Nagasaki University, Nagasaki, Japan

[2]High Medical School, Faculty of Medicine
and Health Care, Al Farabi Kazakh National
University, Almaty, Kazakhstan

[3]Department of Molecular Medicine, Atomic
Bomb Disease Institute, Nagasaki University,
Nagasaki, Japan

[4]Department of Pathology, National
Hospital Organization Nagasaki Medical
Center, Omura, Japan

Correspondence
Yuji Nagayama, Department of Molecular
Medicine, Atomic Bomb Disease Institute,
Nagasaki University, Nagasaki, Japan.
Email: nagayama@nagasaki-u.ac.jp

Abstract

Oncocytic cell tumor of the thyroid is composed of large polygonal cells with eo-sinophilic cytoplasm that is rich in mitochondria. These tumors frequently have the mutations in mitochondrial DNA encoding the mitochondrial electron transport system complex I. However, the mechanism for accumulation of abnormal mitochondria is unknown. A noncanonical mitophagy system has recently been identified, and mitochondria-eating protein (MIEAP) plays a key role in this system. We therefore hypothesized that accumulation of abnormal mitochondria could be attributed to defective MIEAP expression in these tumors. We first show that MIEAP was expressed in all the conventional thyroid follicular adenomas (FAs)/adenomatous goiters (AGs) but not in oncocytic FAs/AGs; its expression was defective not only in oncocytic thyroid cancers but also in the majority of conventional thyroid cancers. Expression of MIEAP was not correlated with methylation status of the 5′-UTR of the gene. Our functional analysis showed that exogenously induced MIEAP, but not PARK2, reduced the amounts of abnormal mitochondria, as indicated by decreased reactive oxygen species levels, mitochondrial DNA / nuclear DNA ratios, and cytoplasmic acidification. Therefore, together with previous studies showing that impaired mitochondrial function triggers compensatory mitochondrial biogenesis that causes an increase in the amounts of mitochondria, we conclude that, in oncocytic cell tumors of the thyroid, increased abnormal mitochondria cannot be efficiently eliminated because of a loss of MIEAP expression, ie impaired MIEAP-mediated noncanonical mitophagy.

KEYWORDS

mitochondria, mitochondria-eating protein, mitophagy, oncocytic cell tumor, thyroid

1 | INTRODUCTION

Thyroid oncocytic cell tumors (also called oxyphilic, eosinophilic, or Hürthle cell tumors) are characterized by the presence of at least 75% oncocytic cells that contain excessive accumulation of abnormally enlarged mitochondria.[1] Although the WHO classification of thyroid tumor currently classifies thyroid oxyphilic cell tumors as an oncocytic variant FA and FTC,[2] they can also be identified in PTCs.[3] Recent genetic/genomic studies have revealed that oncocytic cell carcinomas have distinct genomic alterations as compared with other forms of thyroid cancers.[1] For example, for nDNA mutations, among genetic mutations that are frequently found in non-oncolytic thyroid papillary and follicular cancers (PTC and FTC), oncocytic cell carcinomas have RAS mutations at a lower frequency (10-15%) as compared to FTC, but no BRAF mutations, RET/PTC rearrangements, or Pax8-PPARγ rearrangements. Nevertheless, approximately 55% of mutations were on RAS/RAF/MAPK and PI3K/AKT/mTOR pathways.[2,4] Chromosome number alterations are more common, loss of heterozygosity across many chromosomes often with genome-wide haploidization, also concomitant with amplification of chromosomes 5, 7, and 12 which contain BRAF and RAS genes.[2,4-7] Unique, potential driver mutations such as ERBB2, NF1, and DAXX, have also been determined.[4,7] For mtDNA mutations, importantly, the mutations in complex I of the electron transport chain have been identified.[4,7,8] A phylogenic study indicated that near-haploid states and mtDNA mutations are early events in oncocytic cell carcinogenesis.[7] Furthermore, transcriptomic analyses have shown that distinct gene and microRNA expression profiles are observed between oncocytic cell carcinomas and conventional differentiated thyroid carcinomas.[2,4,5,7,9] Thus it is generally recognized that oncocytic cell tumors represent a distinct class of thyroid tumor at the genetic/genomic levels. Clinically, oncocytic cell carcinomas rarely take up radioiodine, preferentially metastasize to the lymph nodes, and have a greater propensity for malignant transformation to anaplastic thyroid cancers than other types of thyroid cancers, with their overall mortality/morbidity rates being higher in some[1,10] but not in other reports.[11,12]

Despite the aforementioned extensive studies, the molecular mechanism(s) for accumulation of abnormal mitochondria remain to be elucidated. Lee and his colleagues have recently identified a loss of function mutation in the PARK2 gene (V380L) in an oncocytic cell carcinoma line XTC.UC1, causing defective canonical mitophagy, a selective degradation pathway of mitochondria by autophagy, but the same mutation has existed only in 1 of 7 oncocytic cell carcinomas.[13] Also mutations in the molecules involved in mitophagy, such as PARK2 and PINK,[14] have not been identified in the exosome sequencing analyses of a large series of oncocytic cell carcinomas.[4,7]

Recently, another noncanonical mitophagy system has been identified, in which MIEAP plays a key role.[15,16] Mitochondria-eating protein is thought to be a tumor suppressor[17] and its expression has been reported to be suppressed by methylation of its 5′-UTR in 9% of colon cancers and 13% of breast cancers.[18,19] However, the role of MIEAP in the pathogenesis of thyroid oncocytic cell tumors has

not yet been studied. We therefore postulated that accumulation of abnormal mitochondria could be attributed to defective MIEAP expression in thyroid oncocytic cell tumors. We first examined expression of MIEAP protein and methylation of the MIEAP gene in thyroid conventional and oncocytic cell tumors and cancer cell lines, including XTC.UC1 cells, and then evaluated the functional significance of induction of MIEAP expression on phenotype of XTC.UC1 cells.

2 | MATERIALS AND METHODS

2.1 | Human thyroid tissues

A total of 95 surgically resected, FFPE thyroid tumors including 38 oncocytic-type tumors (33 FAs, 5 AGs, 1 FTC, and 2 PTCs) and 54 conventional-type tumors (38 FAs and 16 PTCs) were used in this study. The diagnoses of all patients were histologically confirmed by pathologists specializing in thyroid oncology (ZM, MI, and MN). This study was retrospectively carried out in accordance with the tenets of the Declaration of Helsinki and approved by the institutional ethical committee for medical research at Nagasaki University Graduate School of Biomedical Sciences (protocol no. 15062617). Following the guidelines of the ethical committee's official informed consent and disclosure system, detailed information regarding the study is available on our website (http://www-sdc.med.nagasaki-u.ac.jp/pathology/research/index.html) in Japanese. Patients were able to opt out of the study by following the instructions on the faculty website. All samples were resected from patients at the Nagasaki University Hospital from 1994 to 2012 or the Nagasaki Medical Center from 2010 to 2012.

2.2 | Hematoxylin-eosin staining and IHC for MIEAP expression in human thyroid tissues

Hematoxylin-eosin staining was carried out as described previously.[20] For IHC, after antigen retrieval by autoclaving for 20 minutes at 120°C in Target Retrieval Solution (pH 9.0) (Dako Cytomation), deparaffinized 4-μm sections were processed with a BOND Polymer Refine Kit (Leica Biosystems), according to the manufacturer's instruction, and were incubated for 2 hours at 37°C with an anti-MIEAP rabbit polyclonal Ab (HPA036854, 1:100 dilution; Sigma-Aldrich) in a humidified chamber. All samples were observed at a magnification of ×200. Samples with clear staining for MIEAP in the cytoplasm were considered MIEAP-positive.

2.3 | Methylation-specific PCR and bisulfite sequencing

Genomic DNA was extracted from tumor areas in FFPE tissues obtained between 2011 and 2012. Tumor areas, identified using a guide slide stained with H&E, were microdissected from each FFPE block

using an 8-μm-thick section and transferred into a tube. Paraffin removal was carried out in 80% xylene; tissues were then washed twice with absolute ethanol, and deparaffinized tissue pieces were centrifuged at 15 000 g for 10 minutes at room temperature. Genomic DNA was extracted using a Maxwell RSC DNA FFPE Kit (Promega) according to the manufacturer's instruction. Extracted DNA was quantified using a NanoDrop ND-1000 spectrophotometer (NanoDrop Technologies).

Methylation-specific PCR and bisulfite sequencing were undertaken according to previous reports.[16,18] The MethylEdge Bisulfite Conversion System Kit (Promega) was used to undertake bisulfite conversion of genomic DNA as described in the user's manual. Commercially available converted methylated and unmethylated human DNAs (Promega) were used as positive and negative controls, respectively, for MSP. Bisulfite converted genomic DNA was amplified using the primers specific to the methylated and unmethylated forms of DNA sequences. The primers used for MSP are 5′-GCGCGTTTTTGGTAGTTAATTC-3′ (forward) and 5′-CAAATTTTCCGCCATCGCTC-3′ (reverse) for methylated sequence, and 5′-GTGTGTGTTTTTGGTAGTTAATTTG-3′ (forward) and 5′-CAAATTTTCCACCATCACTCAC-3′ (reverse) for unmethylated sequence. The MSP reaction was carried out using an EpiTect MSP Kit and Master Mix for MSP (Qiagen) in the following conditions: 1 cycle at 95°C for 2 minutes, 45 cycles at 95°C for 30 seconds, 53°C for 30 seconds and 72°C for 1 minute, and a final extension step at 72°C for 10 minutes. The PCR products were visualized on 1.5% agarose gels stained with ethidium bromide. Bisulfite sequencing was carried out with the forward and reverse primers mentioned above with an ABI PRISM 3730 genetic analyzer (Applied Biosystems, Life Technologies) and repeated in total 4 times to confirm results.

2.4 | Cell lines used

An oncocytic carcinoma cell line of the thyroid, XTC.UC1, was established from a metastasis of an oncocytic cell carcinoma in 1998 by Zielke et al,[10] and was obtained from Porcelli AM (University of Bologna, Italy).[21] Conventional, differentiated thyroid cancer cell lines (WRO [derived from a follicular thyroid cancer], and TPC1 and KTC1 [derived from papillary thyroid cancers]) were previously obtained from Fagin JA (Memorial Sloan-Kettering Cancer Center).[22] All the cell lines have wt p53.[23-25] A human hepatocellular carcinoma cell line HepG2 was obtained from RIKEN BioResource Research Center. The cells were cultured in DMEM supplemented with 10% FBS and 1% antibiotics.

X-ray was given as a single dose of 10 Gy at a dose rate of 0.8903 Gy/minute using the ISOVOLT Titan 320 (GE Inspection).

2.5 | Transduction of MIEAP and PARK2 cDNAs into XTC.UC1 cells

MIEAP and PARK2 cDNAs were obtained from RIKEN BioResource Research Center. PARK2 cDNA in frame with the V5 epitope tag was

generated by using KOD-Plus-Mutagenesis Kit (TOYOBO) and was then ligated into the retroviral vector pMSCVneo (Takara-Clontech). MIEAP cDNA was ligated into pMSCVpuro (Takara-Clontech). The resultant vectors pMSCV-PARK2 and pMSCV-MIEAP were transfected into a 293GPG packaging cell line.[26] XTC.UC1 cells were infected with the virus-containing supernatants in the presence of 8 μg/mL polybrene. The infected cells were then selected with G418 and puromycin for PARK2 and MIEAP, respectively, and the bulks of antibiotic-resistant cells were used in the subsequent experiments.

2.6 | Immunofluorescence (IF) for MIEAP, PARK2, and TOMM20 expression in XTC.UC1 and HepG2 cells

The cells were fixed with 3.7% formaldehyde for 10 minutes followed by permeabilization with 0.5% Triton-X and then were incubated with a primary Ab at 4°C overnight. The primary Abs used were rabbit polyclonal anti-MIEAP (HPA036854; 1:100 dilution), rabbit polyclonal anti-PARK2 (HPA036012, 1:25 dilution; Merck), or mouse monoclonal anti-TOMM20 (ab56783, 1:250 dilution; Abcam). Next day, the cells were washed with TBS-T and were incubated with a secondary Ab for 1 hour at room temperature. Secondary Abs used were Alexa Fluor 488 goat anti-rabbit IgG (A-11001, 1:200 dilution; Life Technologies) for anti-MIEAP and anti-PARK2 and Alexa Fluor 594 goat anti-mouse IgG (A-11012, 1:200 dilution; Life Technologies). The cells were washed with TBS-T, and were embedded with VECTASHIELD Mounting Medium containing DAPI (Vector Laboratories). The slides were analyzed using an All-in-One BZ-9000 Fluorescence Microscope (Keyence).

2.7 | Western blot analysis

Forty micrograms of total cell lysates prepared from XTC.UC1, XTC.UC1/MIEAP, and XTC.UC1/PARK2 cells was separated in a gradient SDS-PAGE, and then transferred onto a PVDF membrane. The membrane was blocked with 5% skim milk at 4°C overnight, washed with TBS-T and were incubated with a primary Ab for 1 hour at room temperature. Primary Abs used were rabbit polyclonal anti-MIEAP (HPA036854; 1:100 dilution), rabbit monoclonal V5-Tag (D3H8Q) (#13202S, 1:1000 dilution; Cell Signaling Technology) and monoclonal mouse anti-β-actin Ab (sc-47778, 1:1000 dilution; Santa Cruz Biotechnology). The membrane was washed with TBS-T, and incubated with a secondary Ab for 30 minutes at room temperature. The secondary Abs used were polyclonal goat anti-rabbit IgG conjugated with HRP (#7074, 1:1000 dilution; Cell Signaling Technology) and polyclonal horse anti-mouse IgG conjugated with HRP (#7076, 1:1000 dilution; Cell Signaling Technology). Signals were developed using Pierce ECL western blotting substrate (Thermo Fisher Scientific) and were then quantified with a FluorChem FC3 sensitive chemiluminescent imaging system (Protein Simple).

TABLE 1 Mitochondria-eating protein (MIEAP) expression determined by immunohistochemistry in conventional and oncocytic thyroid follicular tumors

	# of samples studied	MIEAP expression[†]			
		Negative	Low	Moderate	High
Conventional FA/AGs	38	0 (0)	0 (0)	6 (16)	32 (84)
Oncocytic FA/AGs	38	29 (76)	9 (24)	0 (0)	0 (0)
Conventional PTCs	16	13 (81)	1 (6)	2 (13)	0 (0)
Oncocytic PTC/FTCs	3	3 (100)	(0)	0 (0)	0 (0)

AG, adenomatous goiter; FA, follicular adenoma; FTC, follicular thyroid cancer; PTC, papillary thyroid cancer.

[†]Data shown as n (%).

2.8 | Reactive oxygen species (superoxide) measurements

Cells (1 × 10^4) were seeded in a 96-well plate and were incubated for 24 hours at 37°C. After washing with PBS, the cells were incubated with 5 μM MitoSOX (Thermo Fisher Scientific) for 30 minutes at 37°C and were washed again with PBS. The plates were then read with 2030 Multilabel Plate Reader ARVO X3 (PerkinElmer) at excitation and emission wavelengths of 510 (excitation) and 590 (emission) nm.

2.9 | Determination of mtDNA to nDNA ratios

Total DNA was extracted from the parental XTC.UC1, XTC.UC1/MIEAP, and XTC.UC1/PARK2 cells using DNeasy Blood & Tissue Kit (Qiagen). Quantitative PCR according to the ΔΔCt method was carried out as described previously.[27,28] *12S rDNA* encoded by mtDNA and *β-actin* encoded by nDNA were quantified, and the mtDNA / nDNA ratio was used to estimate the relative mtDNA copy number, ie the relative amounts of mitochondria. *12Sr* DNA primers are 5′-TAACCCAAGTCAATAGAAGCC-3′ and 5′-CTAGAGGGATATGAAGCACC-3′, and human *β-actin* primers are 5′-GAGCGGGAAATCGTGCGTGAC-3′ and 5′-GGAAGGAAGGCTGGAAGAGTG-3′.

2.10 | Cell viability assay

Cells (1 × 10^3) were seeded in a 96-well plate, and were incubated at 37°C. Cell viability was then measured 24 and 72 hours later with CCK-8 (Dojindo) in accordance with the manufacturer's protocol.

2.11 | In vivo tumor model

The cell suspension (1 × 10^6 cells/ 100 μL PBS) was injected s.c. into 6-week-old male BALB/c nu/nu mice (Charles River Japan). Tumor size was measured with a caliper once a week, and tumor volume was calculated according to the formula: $a^2 \times b \times 0.4$, where a is the smallest tumor diameter and b is the diameter perpendicular to a. Mice were killed when b reached approximately 1 cm.

2.12 | Hematoxylin-eosin and immunofluorescence for Ki-67 and TUNEL staining in XTC.UC1 and XTC.UC1/MIEAP tumors

XTC.UC1 and XTC.UC1/MIEAP tumors were excised and fixed in 10% neutral-buffered formalin and embedded in paraffin. Staining with H&E was carried out as mentioned above. For Ki-67 staining, 4-μm sections were treated with 3% hydrogen peroxide to block endogenous peroxidase and subjected to antigen retrieval by microwave treatment in citrate buffer, followed by incubation with rabbit polyclonal anti-Ki-67 Ab (ab66155, 1:200 dilution; Abcam) and then with Alexa Fluor 488-conjugated goat polyclonal anti-rabbit IgG (A-11008, 1:200 dilution; Life Technologies). The slides were then analyzed with an All-in-one Fluorescence Microscope BZ-9000 (Keyence). One hundred cells were evaluated to determine the percentage of Ki67-positive cells (n = 4).

The TUNEL staining was carried out with the Apop-tag Fluorescein Direct in situ apoptosis detection kit (Merck Millipore). The slides were embedded with VECTASHIELD Mounting Medium containing DAPI (Vector Laboratories) and analyzed using an All-in-One BZ-9000 fluorescence microscope. One hundred cells were evaluated in each sample (n = 4) to determine the percentages of TUNEL-positive cells.

2.13 | Statistical analysis

All data were analyzed by Student's *t* test. A *P* value of less than .05 was considered statistically significant.

3 | RESULTS

3.1 | Immunohistochemistry for MIEAP expression

The results of IHC analysis of MIEAP expression in thyroid tumors are summarized in Table 1, and the representative photographs are

depicted in Figure 1. All conventional FAs and AGs (38/38, 100%) were positive (moderate to high), whereas oncocytic tumors (38/38, 100%) were negative or only weakly positive, for MIEAP expression. However, MIEAP expression was defective not only in 3 of 3 (100%) oncocytic carcinomas but also in 13 of 16 (81%) conventional carcinomas. Most normal follicular epithelia were MIEAP-positive, although expression was heterogeneous. In cell lines, MIEAP immunoreactivity was found in HepG2 (used as a positive control) but not in any thyroid cancer cell lines, including oncocytic carcinoma cell line XTC.UC1 (Figure 1). Thus, the data obtained with benign thyroid FAs/AGs, but not cancers, support our hypothesis.

3.2 | Methylation status of 5′-UTR of *MIEAP*

Expression of MIEAP is TP53-dependent[16] and suppressed by gene methylation in several cancers with intact TP53.[16] As TP53 is largely intact in differentiated thyroid cancers,[29] methylation status of the 5′-UTR of the *MIEAP* gene was analyzed by MSP and was verified by bisulfite sequencing. We focused on approximately 300 bp of the

5′-UTR of the *MIEAP* gene, because a clear correlation between the methylation status of this region and MIEAP expression has been reported in colon and breast cancers.[18,19] CpG sites and locations of MSP primers are shown in Figure S1. The FFPE samples that met the DNA quality standard were used for these experiments (20 conventional and 14 oncocytic FAs). The DNA quality standard was provided in the protocol for the MethylEdge Bisulfite Conversion System (Promega), in which the NanoDrop spectrophotometer was set to "DNA-50" for DNA extracted from FFPE and to "RNA-40" for bisulfite-converted DNA. In MSP, unexpectedly, the methylated DNAs were detected in approximately half of both conventional and oncocytic FAs (8/20 [40%] and 6/14 [43%], respectively) (Table 2). The representative data (3 samples for each group) are shown in Figure S2A (right panel). Furthermore, the direct sequencing with bisulfite genomic DNA confirmed the methylated CpG sites in each case (Figure S2A, black boxes). Thus, defective expression of MIEAP in oncocytic FAs cannot be explained by the methylation status of the *MIEAP* gene. However, of interest, careful comparison of the methylation status in the *MIEAP* gene and pathological features in oncocytic FAs revealed that oncocytic FAs with the methylated
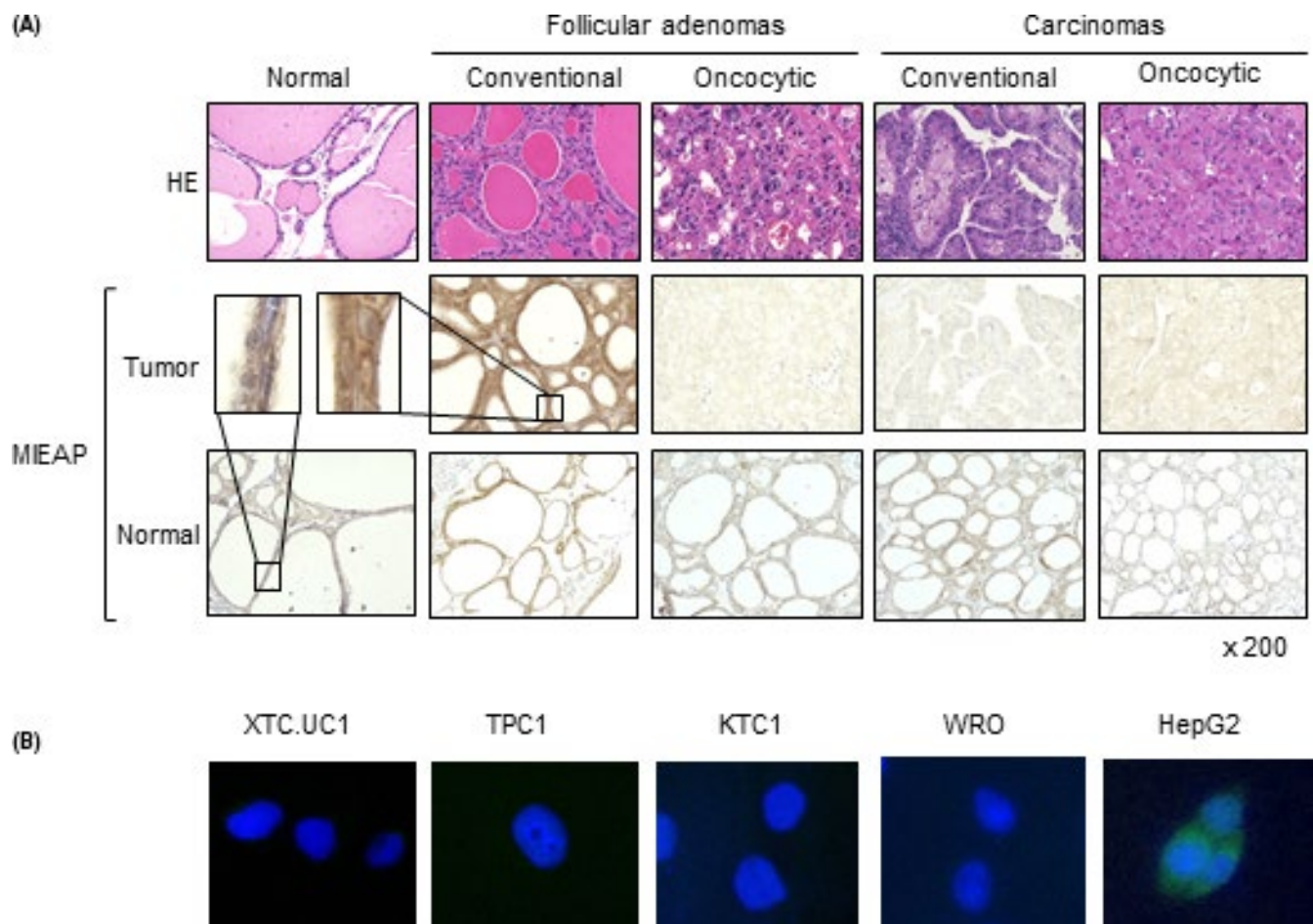

FIGURE 1 Hematoxylin-eosin staining and immunohistochemistry (IHC) for mitochondria-eating protein (MIEAP) expression in thyroid tissues, and immunofluorescence (IF) for MIEAP in thyroid cancer cell lines and HepG2 cells. Human thyroid tissues and cell lines were subjected to H&E staining and/or MIEAP IHC/IF staining. Representative photographs of H&E and MIEAP staining in normal tissue, conventional and oncocytic follicular adenomas and carcinomas, and cell lines. The photographs of MIEAP expression in tumorous and normal regions were taken from the same samples (A). Original magnifications, ×200 (A) and ×400 (B)

	Gene methylation	
	Unmethylated	**Methylated**
Oncocytic FAs	8/14 (57%)	6/14 (43%)
Conventional FAs	12/20 (60%)	8/20 (40%)

MIEAP gene have more enlarged cytoplasm and characteristic nuclear features such as higher nucleic polymorphism, more prominent nuclei, and more frequent pyknotic nuclei (ie prominent oncocytic features) than those with the unmethylated gene (Figure S3).

The *MIEAP* gene was heavily methylated in oncocytic XTC.UC1 cells, as determined by MSP and bisulfide sequencing, and also conventional cancer cell lines by MSP (Figure S2B). In contrast, unmethylated status has previously been reported in HepG2 cells.[16]

3.3 | Effect of reexpression of MIEAP and PARK2 in XTC.UC1 cells

Next, mechanistic studies on the functional role for MIEAP-mediated mitochondrial quality control in oncocytic cell tumors were undertaken with XTC.UC1 cells, because these cells are the only available oncocytic tumor cell line. Because these cells not only have defective MIEAP expression, as shown in Figure 1, but also harbor a loss-of-function mutant PARK2,[13] we tried to express MIEAP and PARK2 in XTC.UC1 cells. Our first attempt to demethylate the *MIEAP* gene with 5-azacytidine, a demethylating agent, failed (Figure S4). Therefore, the *MIEAP* and *PARK2-V5* genes were retrovirally transduced into XTC.UC1 cells. Western blot analysis clearly detected expression of MIEAP with anti-MIEAP Ab (61.1 kDa) and of V5-tagged PARK2 (53.0 kDa; 51.6 kDa PARK2 + 1.4 kDa V5 epitope) with anti-V5 Ab in the cells transduced with *MIEAP* and *PARK2* cDNAs, respectively (hereafter XTC.UC1/MIEAP and MIEAP/PARK2 cells) (Figure 2A,C). Immunohistochemistry indicated that MIEAP and PARK2 expression was colocalized with TOMM20, a mitochondrial outer membrane protein (Figure 2B,D), indicating that these molecules were recruited to mitochondria, exerting their roles in canonical and noncanonical mitophagy.

To determine whether MIEAP and PARK expressed in XTC.UC1 cells participate in mitochondrial quality control by eliminating abnormal mitochondria, the amounts of mitochondria and of mitochondrial ROS (superoxide) were determined with mtDNA / nDNA ratios and MitoSOX staining, respectively, and were then compared among the parental XTC.UC1, XTC.UC1/MIEAP, and XTC.UC1/PARK2 cells. As shown in Figure 2E,F, introduction of MIEAP significantly reduced ROS levels and mtDNA / nDNA ratios, that is, MIEAP reduced the amounts of abnormal mitochondria producing excess ROS. Introduction of PARK2 is less efficient, showing only insignificant reduction of the amounts of mitochondria. In addition, to determine whether MIEAP reexpression changes the H&E staining pattern, the parental XTC.UC1 and XTC.UC1/MIEAP cells were

inoculated s.c. into nude mice. We first found that MIEAP reexpression significantly reduced in vitro cell growth and in vivo tumor growth of XTC.UC1/MIEAP cells as compared with the parental cells (Figure 3A, B). Simultaneous H&E staining clearly showed that eosinophilic cytoplasm of XTC.UC1 tumors faded away by MIEAP reexpression as compared with XTC.UC1 tumors (Figure 3C). Ki-67 and TUNEL staining (shown in Figure 3D) indicates that reduced in vivo tumor growth was due to higher apoptotic cell death, not lower proliferative rate, of XTC.UC1/MIEAP tumors as compared with XTC.UC1 tumors.

4 | DISCUSSION

MIEAP, also known as spermatogenesis associated 18 (SPATA18) in humans, was originally identified as a TP53-inducing molecule.[16,30] Its expression is suppressed by methylation of the 5′-UTR of the *MIEAP* gene or TP53 loss-of-function mutations in colorectal and breast cancers.[16,18,19] Although MIEAP expression status is not correlated with clinicopathologic parameters in colorectal cancers,[18] it is positively associated with aggressiveness, and negatively with disease-free survival in breast cancers.[19] Functionally, MIEAP plays a role in mitochondrial quality control, and thus its defective expression causes accumulation of unhealthy mitochondria and elevated ROS levels.[31] Mitochondria-eating protein exerts its function by either repairing or eliminating unhealthy mitochondria through the mechanisms of "MIEAP-induced accumulation of lysosome-like organelles within mitochondria" (fixing unhealthy mitochondria by removing oxidized mitochondrial proteins) or "MIEAP-induced vacuole" (eliminating abnormal mitochondria), respectively.[16,32] Although *MIEAP* KO mice are healthy, defective MIEAP expression accelerated and aggravated intestinal tumors and shortened lifespan in *Apc*[Min/+] mice.[17] Furthermore, abrogation of MIEAP expression enhanced the migratory and invasive ability of a colorectal cancer cell line in hypoxic conditions (another inducer of MIEAP).[18] Forced overexpression of exogenous MIEAP induced MIEAP-induced vacuole and apoptotic cell death in some breast cancer cell lines,[19] and a MIEAP-nonexpressing gastric cancer cell line produced more ROS and was more invasive in hypoxic conditions than a MIEAP-expressing one.[33] By contrast, it is also reported that MIEAP participates in the hypoxic process of voltage-dependent anion-selective channel 1 and chemoresistance.[34]

In this study, we sought to prove our hypothesis that accumulation of abnormal mitochondria could be attributed to defective MIEAP expression in thyroid oncocytic cell tumors. Our IHC analyses of MIEAP expression clearly indicates that MIEAP expression is absent exclusively in oncocytic, not in conventional, benign FAs/AGs. However, although defective MIEAP expression is solely due to the *MIEAP* gene methylation in colorectal and breast cancers with intact TP53,[18,19] we found no correlation between MIEAP expression and the *MIEAP* gene methylation status in conventional and oncocytic FAs/AGs. Thus, expression levels of MIEAP cannot simply be explained by the gene methylation
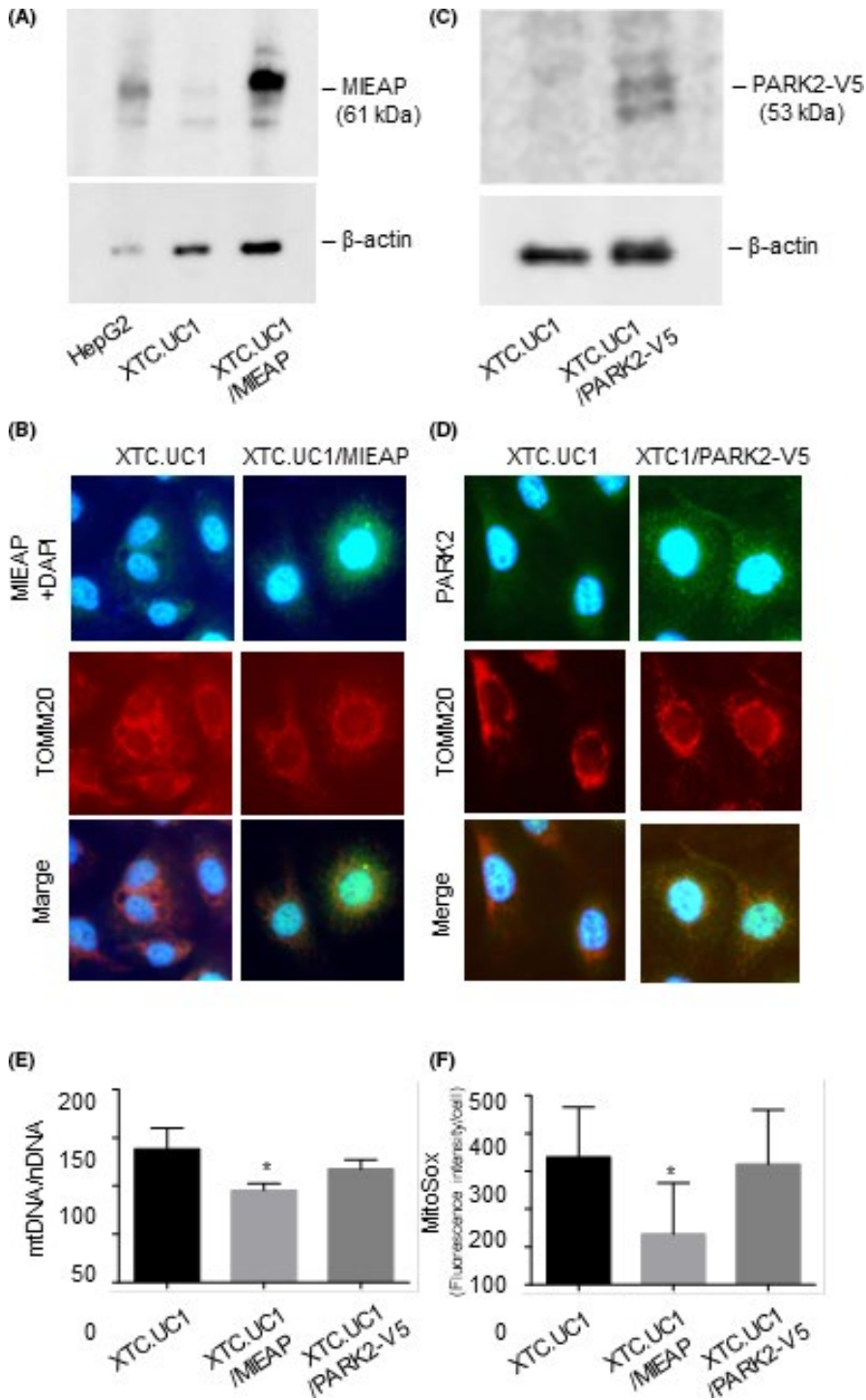
FIGURE 2 Expression and localization of mitochondria-eating protein (MIEAP) and PARK2, the amounts of mitochondria and ROS in parental and MIEAP or PARK2-expressing XTC.UC1 cells. A, C, *MIEAP* and *PARK2-V5* cDNAs were retrovirally transduced into XTC.UC1 cells and their expression was confirmed in WB. B, D, Colocalization of MIEAP or PARK2 and mitochondria was evaluated by staining with anti-MIEAP, -PARK2, and -TOMM20 Abs, and DAPI. E, F, Amounts of mitochondria and reactive oxygen species levels were determined with mitochondrial DNA (mtDNA) / nuclear DNA (nDNA) ratios and MitoSOX, respectively. Data are means ± SD (n = 4). *P < .05 compared to control. Original magnifications, ×400 (B)

status in thyroid tumors. Recent methylome studies have revealed that DNA methylation in promoter regions does not have a widespread role in controlling gene expression in PTCs.[35] However, of interest, as shown in Table 2 and Figure S3, the methylation of the *MIEAP* gene was detected in oncocytic FAs with prominent oncocytic features, not in those without. There could be 2 possibilities to explain these data. The first is that the mechanisms for MIEAP suppression are different between these 2 subgroups, ie suppression is methylation-dependent in the former but methylation-independent in the latter. The second is that, assuming that

the latter gradually progresses to the former, MIEAP expression is suppressed by nonmethylation mechanism(s) in the latter and then, during progression, methylation occurs in the *MIEAP* gene of the former; in this regard, methylation is functionally irrelevant.

In contrast to benign FAs/AGs, the difference in MIEAP expression status was not observed between conventional vs oncocytic carcinomas. Although only a very small number of oncocytic carcinomas was available, which is a limitation of this study, an important finding is defective MIEAP expression, even in more than 80% of conventional PTCs.

FIGURE 3 In vivo and in vitro growth of parental XTC.UC1 and XTC.UC1/ MIEAP cells, and H&E staining of XTC. UC1 and XTC.UC1/mitochondria-eating protein (MIEAP) tumors. A, B, In vitro and in vivo growth of cells were determined. Closed circles and squares indicate the data obtained with XTC.UC1 and XTC. UC1/MIEAP cells, respectively. Data are means ± SE (n = 3-4). *P < .05 compared to parental cells. C, H&E staining of tumors formed in (B). Original magnification, ×100. D, Number of Ki67-positive cells and TUNEL-positive cells in tumors formed in (A). *P < .05. NS, not significant
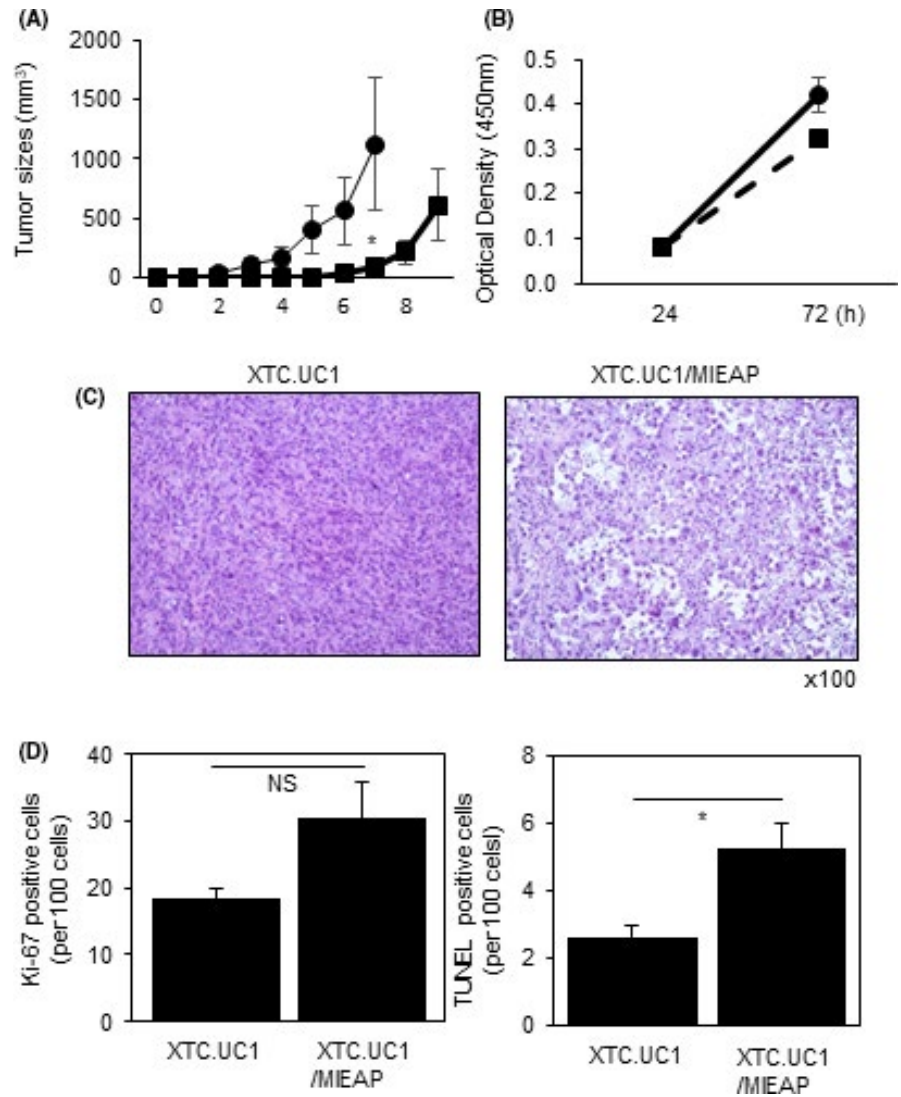
Functional studies on the significance of mitochondrial quality control in mitochondrial turnover were then carried out with XTC.UC1 cells. In this cell line, defective mitochondrial function has long been described,[36] and homoplastic mtDNA mutations (a frameshift mutation of ND1 [a C insertion at bp3571, generating a premature stop codon at a.a. 101 in the ND1 subunit of complex I and a truncated ND1 protein] and a nonconservative E271K substitution [due to 15557G > A] in the cytochrome *b* gene) have previously been detected.[21,37] More recently, Shong and his colleagues have identified a loss of function mutation in the *PARK2* gene, a critical molecule for canonical mitophagy, in this cell line.[13] This mutation has been detected in familial Parkinson's disease. In our studies, reexpression of MIEAP efficiently eliminated abnormal mitochondria, as indicated by reduced ROS and mtDNA / nDNA ratios in vitro and reduced eosinophilic staining in vivo, whereas the effect of PARK2 was insignificant. Thus, these data support our hypothesis that MIEAP plays a significant role in mitochondrial quality control in oncocytic tumor cells. However, Shong et al[13] have recently reported the significant acceleration of mitochondrial turnover by PARK2 expression in XTC.UC1 cells. Although the reason for these inconsistent data is at present unknown, endogenous PARK2 is constitutively expressed in a physiological condition, whereas MIEAP expression is low at the basal level and is induced by TP53. Our XTC.UC1/MIEAP cells expressed high levels of exogenous MIEAP constitutively. Thus, we do not want to emphasize our data showing the higher efficacy of mitochondrial turnover by MIEAP than PARK2 in our experimental setting. Presumably both types of mitophagy (canonical and noncanonical) more or less similarly contribute to efficient mitochondrial turnover. In fact, induction of the oncocytic phenotype by *Atg5* or *Atg7* KO (inducing defective canonical mitophagy) has been reported in mouse lung tumor models using *LSL-K-ras*[G12D] or *Braf*[CA] mice treated intranasally with adenoviral Cre DNA recombinase.[38-40] In contrast, canonical mitophagy is a very rapid process and is completed within a few hours, whereas MIEAP-mediated non-canonical mitochondrial quality control is a slow process and continues for days.[15] As oncocytic tumor cells continuously produce abnormal mitochondria, it is possible that MIEAP-mediated noncanonical mitophagy is more important than PARK2-mediated canonical mitophagy for turnover of persistently produced abnormal mitochondria.

Finally, together with previous studies showing that impaired mitochondrial function triggers compensatory mitochondrial

biogenesis that causes the accumulation of mitochondria,[13,41] we would like to conclude that, in oncocytic cell tumors of the thyroid, increased abnormal mitochondria cannot efficiently be eliminated because of a loss of MIEAP expression, ie a defect in MIEAP-mediated noncanonical mitophagy. However, further study will definitely be necessary to elucidate the mechanism for suppression of MIEAP expression other than gene methylation and also the relevance of defective MIEAP expression in conventional cancers with intact mitochondria.

CONFLICT OF INTEREST

The authors have no conflict of interest.

ORCID

Yuji Nagayama https://orcid.org/0000-0002-5058-9349

REFERENCES

1. Ganly I, McFadden DG. Short review: genomic alterations in hurthle cell carcinoma. *Thyroid*. 2019;29:471-479.
2. Ganly I, Ricarte Filho J, Eng S, et al. Genomic dissection of Hurthle cell carcinoma reveals a unique class of thyroid malignancy. *J Clin Enodocrinol Metab*. 2013;98:E962-972.
3. Cavadas B, Pereira JB, Correia M, et al. Genomic and transcriptomic characterization of the mitochondrial-rich oncocytic phenotype on a thyroid carcinoma background. *Mitochondrion*. 2019;46:123-133.
4. Ganly I, Makarov V, Deraje S, et al. Integrated genomic analysis of hurthle cell cancer reveals oncogenic drivers, recurrent mitochondrial mutations, and unique chromosomal landscapes. *Cancer Cell*. 2018;34:256-270. e255.
5. Kurelac I, de Biase D, Calabrese C, et al. High-resolution genomic profiling of thyroid lesions uncovers preferential copy number gains affecting mitochondrial biogenesis loci in the oncocytic variants. *Am J Cancer Res*. 2015;5:1954-1971.
6. Corver WE, Ruano D, Weijers K, et al. Genome haploidisation with chromosome 7 retention in oncocytic follicular thyroid carcinoma. *PLoS One*. 2012;7:e38287.
7. Gopal RK, Kubler K, Calvo SE, et al. Widespread chromosomal losses and mitochondrial DNA alterations as genetic drivers in hurthle cell carcinoma. *Cancer Cell*. 2018;34:242-255. e245.
8. Gasparre G, Porcelli AM, Bonora E, et al. Disruptive mitochondrial DNA mutations in complex I subunits are markers of oncocytic phenotype in thyroid tumors. *Proc Nat Acad Sci USA*. 2007;104:9001-9006.
9. Dettmer M, Vogetseder A, Durso MB, et al. MicroRNA expression array identifies novel diagnostic markers for conventional and oncocytic follicular thyroid carcinomas. *J Clin Endocrinol Metab*. 2013;98:E1-7.
10. Zielke A, Tezelman S, Jossart GH, et al. Establishment of a highly differentiated thyroid cancer cell line of Hurthle cell origin. *Thyroid*. 1998;8:475-483.
11. Maximo V, Lima J, Prazeres H, Soares P, Sobrinho-Simoes M. The biology and the genetics of Hurthle cell tumors of the thyroid. *Endocr Relat Cancer*. 2012;19:R131-147.
12. Evans HL, Vassilopoulou-Sellin R. Follicular and Hurthle cell carcinomas of the thyroid: a comparative study. *Am J Surg Pathol*. 1998;22:1512-1520.
13. Lee J, Ham S, Lee MH, et al. Dysregulation of Parkin-mediated mitophagy in thyroid Hurthle cell tumors. *Carcinogenesis*. 2015;36:1407-1418.
14. Um JH, Yun J. Emerging role of mitophagy in human diseases and physiology. *BMB Rep*. 2017;50:299-307.
15. Nakamura Y, Arakawa H. Discovery of Mieap-regulated mitochondrial quality control as a new function of tumor suppressor p53. *Cancer Sci*. 2017;108:809-817.
16. Miyamoto Y, Kitamura N, Nakamura Y, et al. Possible existence of lysosome-like organella within mitochondria and its role in mitochondrial quality control. *PLoS One*. 2011;6:e16054.
17. Tsuneki M, Nakamura Y, Kinjo T, Nakanishi R, Arakawa H. Mieap suppresses murine intestinal tumor via its mitochondrial quality control. *Sci Rep*. 2015;5:12472.
18. Kamino H, Nakamura Y, Tsuneki M, et al. Mieap-regulated mitochondrial quality control is frequently inactivated in human colorectal cancer. *Oncogenesis*. 2016;4:e181.
19. Gaowa S, Futamura M, Tsuneki M, et al. Possible role of p53/Mieap-regulated mitochondrial quality control as a tumor suppressor in human breast cancer. *Cancer Sci*. 2018;109:3910-3920.
20. Kurashige T, Nakajima Y, Shimamura M, et al. Basal autophagy deficiency causes thyroid follicular epithelial cell death in mice. *Endocrinology*. 2019;160:2085-2092.
21. Bonora E, Porcelli AM, Gasparre G, et al. Defective oxidative phosphorylation in thyroid oncocytic carcinoma is associated with pathogenic mitochondrial DNA mutations affecting complexes I and III. *Cancer Res*. 2006;66:6087-6096.
22. Shimamura M, Nagayama Y, Matsuse M, Yamashita S, Mitsutake N. Analysis of multiple markers for cancer stem-like cells in human thyroid carcinoma cell lines. *Endocr J*. 2014;61:481-490.
23. Kurebayashi J, Tanaka K, Otsuki T, et al. All-trans-retinoic acid modulates expression levels of thyroglobulin and cytokines in a new human poorly differentiated papillary thyroid carcinoma cell line, KTC-1. *J Clin Endocrinol Metab*. 2000;85:2889-2896.
24. Morani F, Phadngam S, Follo C, et al. PTEN deficiency and mutant p53 confer glucose-addiction to thyroid cancer cells: impact of glucose depletion on cell proliferation, cell survival, autophagy and cell migration. *Genes Cancer*. 2014;5:226-239.
25. Messina RL, Sanfilippo M, Vella V, et al. Reactivation of p53 mutants by prima-1 [corrected] in thyroid cancer cells. *Int J Cancer*. 2012;130:2259-2270.
26. Ory DS, Neugeboren BA, Mulligan RC. A stable human-derived packaging cell line for production of high titer retrovirus/vesicular stomatitis virus G pseudotypes. *Proc Nat Acad Sci USA*. 1996;93:11400-11406.
27. Zhang R, Wang J. HuR stabilizes TFAM mRNA in an ATM/p38-dependent manner in ionizing irradiated cancer cells. *Cancer Sci*. 2018;109:2446-2457.
28. Shimamura M, Yamamoto K, Kurashige T, Nagayama Y. Intracellular redox status controls spherogenicity, an in vitro cancer stem cell marker, in thyroid cancer cell lines. *Exp Cell Res*. 2018;370:699-707.
29. The Cancer Genome Atlas Research Network. Integrated genomic characterization of papillary thyroid carcinoma. *Cell*. 2014;159:676-690.
30. Bornstein C, Brosh R, Molchadsky A, et al. SPATA18, a spermatogenesis-associated gene, is a novel transcriptional target of p53 and p63. *Mol Cell Biol*. 2011;31:1679-1689.
31. Kitamura N, Nakamura Y, Miyamoto Y, et al. Mieap, a p53-inducible protein, controls mitochondrial quality by repairing or eliminating unhealthy mitochondria. *PLoS One*. 2011;6:e16060.
32. Nakamura Y, Kitamura N, Shinogi D, et al. BNIP3 and NIX mediate Mieap-induced accumulation of lysosomal proteins within mitochondria. *PLoS One*. 2012;7:e30767.
33. Okuyama K, Kitajima Y, Egawa N, et al. Mieap-induced accumulation of lysosomes within mitochondria (MALM) regulates gastric

cancer cell invasion under hypoxia by suppressing reactive oxygen species accumulation. *Sci Rep.* 2019;9:2822.

34. Brahimi-Horn MC, Lacas-Gervais S, Adaixo R, et al. Local mitochondrial-endolysosomal microfusion cleaves voltage-dependent anion channel 1 to promote survival in hypoxia. *Mol Cell Biol.* 2015;35:1491-1505.

35. Zafon Llopis C, Gil J, Perez-Gonzalez B, Jorda M. DNA methylation in thyroid cancer. *Endocr Relat Cancer.* 2019;26:R415-R439.

36. Savagner F, Chevrollier A, Loiseau D, et al. Mitochondrial activity in XTC.UC1 cells derived from thyroid oncocytoma. *Thyroid.* 2001;11:327-333.

37. Porcelli AM, Ghelli A, Ceccarelli C, et al. The genetic and metabolic signature of oncocytic transformation implicates HIF1alpha destabilization. *Hum Mol Genet.* 2010;19:1019-1032.

38. Guo JY, Karsli-Uzunbas G, Mathew R, et al. Autophagy suppresses progression of K-ras-induced lung tumors to oncocytomas and maintains lipid homeostasis. *Genes Dev.* 2013;27:1447-1461.

39. Strohecker AM, Guo JY, Karsli-Uzunbas G, et al. Autophagy sustains mitochondrial glutamine metabolism and growth of BrafV600E-driven lung tumors. *Cancer Discov.* 2013;3:1272-1285.

40. Rao S, Tortola L, Perlot T, et al. A dual role for autophagy in a murine model of lung cancer. *Nat Commun.* 2014;5:3056.

41. Gasparre G, Romeo G, Rugolo M, Porcelli AM. Learning from oncocytic tumors: why choose inefficient mitochondria? *Biochim Biophys Acta.* 2011;1807:633-642.

SUPPORTING INFORMATION

Additional supporting information may be found online in the Supporting Information section.